Production of meson molecules in ultraperipheral heavy ion collisons

F. C. Sobrinho,[1] L. M. Abreu,[1,2] C. A. Bertulani,[3,4] and F. S. Navarra[1]

[1]*Instituto de Física, Universidade de São Paulo, Rua do Matão 1371—CEP 05508-090, Cidade Universitária, São Paulo, São Paulo, Brazil*

[2]*Instituto de Física, Universidade Federal da Bahia, Campus Ondina, Salvador, Bahia 40170-115, Brazil*

[3]*Department of Physics and Astronomy, Texas A&M University-Commerce, Commerce, Texas 75429, USA*

[4]*Institut für Kernphysik, Technische Universität Darmstadt, 64289 Darmstadt, Germany*

(Received 15 May 2024; accepted 5 August 2024; published 30 August 2024)

In this work we present a calculation of exotic charmonium production in ultraperipheral collisions, in which the exotic state is explicitly treated as a meson molecule. Our formalism is general, but we focus on the lightest possible exotic charmonium state: a D^+D^- molecular bound state. It was proposed some time ago, and it has been an object of experimental searches. Here we study the production of the open charm pair in the process $\gamma\gamma \to D^+D^-$. Then we use a prescription to project the free pair $|D^+D^-\rangle$ onto a bound state at the amplitude level and compute the cross section of the process $\gamma\gamma \to B$ (where B is the bound state). Finally, we convolute this last cross section with the equivalent photon distributions coming from the projectile and target in an ultraperipheral collision and find the $AA \to AAB$ cross section, which, for $Pb-Pb$ collisions at $\sqrt{s_{NN}} = 5.02$ TeV, is of the order of 3 μb.

DOI: 10.1103/PhysRevD.110.034037

I. INTRODUCTION

One of the most important research topics in modern hadron physics is the study of the exotic heavy quarkonium states [1,2]. These new mesonic states are not conventional $c\bar{c}$ configurations, and their minimum quark content is $c\bar{c}q\bar{q}$. This leads us to the main question in the field: are these multiquark states compact tetraquarks, or are they meson molecules? So far there is no conclusive answer. One can try to address this question with the help of experiment and study the observables: masses, decay widths, and production rates. How can multiquark states be produced? They can be produced in B decays and in e^+e^-, proton-proton, proton-nucleus, and nucleus-nucleus collisions. We will focus on the latter, which can be divided into central (and semicentral) and ultraperipherals (UPCs) [3]. In UPCs the nuclei do not overlap, and there are only a few particles produced. In these collisions the elementary processes which contribute to particle production are photon-photon, photon-Pomeron, and Pomeron-Pomeron fusion. The advantage of UPCs is the low particle-production multiplicity, thus with a reduced background if proper detection techniques are used. Such features have been explored at the large hadron collider (LHC) at CERN and at the relativistic heavy ion collider at Brookhaven. In this work we will study exotic charmonium (assumed to be a meson molecule) in photon-photon processes in ultra-peripheral nucleus-nucleus collisions. We will compare our results with those obtained in previous studies [4,5] along the same line.

Coming back to the question formulated above, the strategy to get the answer is to compute the cross section for production (in UPCs) of a given exotic charmonium state assuming that it is (i) a tetraquark and also assuming that it is (ii) a meson molecule. There are reasons to believe that the resulting cross sections are very different from each other, and hence, just looking at the production rate, one could experimentally discriminate between the two configurations. In Refs. [4,5], the resonance (R) production via photon-photon fusion was studied, and several cross sections were obtained. In that work the authors used the Low formula, in which the $\gamma\gamma \to R$ cross section is proportional to the $R \to \gamma\gamma$ decay width, $\Gamma_{\gamma\gamma}$. This last quantity depends on the value of the wave function at the origin $|\psi(0)|^2$, which is expected to be much larger for compact tetraquarks than for loosely bound extended meson molecules. Based on this argument we might expect that the production cross section of tetraquarks would be larger than the one for molecules. In [4,5] the authors needed $\Gamma_{\gamma\gamma}$ as input. Unfortunately, this width was only measured in very few cases. In some other very few cases the width was estimated with the help of a formalism valid

for states dynamically generated in meson-meson interactions. By construction, these are molecular states. Here we propose a method to form the molecular state which is more general and independent of the knowledge of the decay width. The method employed here is applicable to all molecular states. Another important difference is in the definition of an ultraperipheral collision. In Refs. [4,5] the authors use a purely geometrical definition, limiting the integration over the impact parameter. Here we follow [6] and define the UPC in momentum space. The study of tetraquark production, which is relevant to the present work has been done in Refs. [7,8] and will be discussed in Sec. VI.

The production of hadron molecules has been discussed in the context of B decays [9], in e^+e^- collisions, in proton-proton [10,11], in proton-nucleus, and in central nucleus-nucleus collisions [12]. We start with the lightest charm meson molecule: the D^+D^- state (also called $D\bar{D}$). It was predicted in the study of meson-meson interactions in the charm sector in [13], where it was found to be bound by about 20 MeV. The state was confirmed in subsequent theoretical studies [14,15]. More recently it was also found in lattice calculations [16]. In [17], it was shown that the peak in the $D\bar{D}$ invariant mass, observed by the BELLE Collaboration [18], could be well explained by the existence of a hidden charm scalar resonance below the threshold [13]. An updated experimental work was performed in [19], and, again, support for the $D\bar{D}$ state in the reaction $e^+e^- \to D\bar{D}$ (and also in $\gamma\gamma \to D\bar{D}$) was found. Recent analyses of these data were published in [20,21]. A more refined theoretical work of these reactions was performed in [22–24], claiming again evidence for this bound state.

The observations of the $D\bar{D}$ state in the low energy machines are crucial to confirm the existence of the state. However they may be not sufficient to determine the internal structure of the state. Here the high energy UPCs can be useful because the intensity of the photon flux grows with the energy, increasing the cross sections and the productions statistics. Hence UPCs offer a complementary way to discriminate between tetraquarks from molecules.

In the next section we present the formalism employed to describe D^+D^- pair production; in Sec. III we present the prescription to create the bound state; in Sec. IV we discuss the equivalent photon spectrum; in Sec. V, performing a low energy approximation, we derive an analytical formula for the cross section of bound state production. In the final section we present numerical results and discussion.

II. PRODUCTION OF FREE D^+D^- PAIRS

There are two ways to produce a D^+D^- from two photons. In the first, one of the photons splits directly into the pair $\gamma \to D^+D^-$, where one of the mesons is already on the mass shell, and the second photon brings the other D to the mass shell. This process can be described by a well-known hadronic effective Lagrangian, from which we obtain the pair production amplitude. This amplitude is subsequently projected onto the amplitude for bound state formation. If the properties of the bound state are known, the only unknown in this formalism is the form factor, which must be attached to the vertices to account for the finite size of the hadrons.

In the second way to produce the pair, one photon splits into a $c\bar{c}$ pair which, after interacting with the second photon, hadronizes into the D^+D^- pair. Then, using a coalescence prescription, we obtain a model for the production of the bound state. The hadronization process involves uncertainties related to its nonperturbative nature. Here we cannot automatically use fragmentation functions, which require a hard scale. Moreover, the coalescence prescription contains some inherent arbitrariness.

In principle using hadronic or partonic degrees of freedom should yield the same results. This is a guiding principle for constructing effective theories. In both approaches there are uncertainties, and depending on the specific observable, it may be more convenient to use one or another approach. In the present case in each approach there is a sequence of steps summarized as follows.

(I) In a QCD based calculation we (i) compute the $\gamma\gamma \to c\bar{c}$ cross section, (ii) use fragmentation functions to include the hadronization of the charm quarks $c \to D$ and $\bar{c} \to \bar{D}$, and (iii) introduce some coalescence model to form the $D\bar{D}$ bound state. Steps (i) and (ii) were executed in the early works [25–28]. Step (iii) was executed much later for the $D\bar{D}^*$ bound state in [29].

(II) In a hadronic description we (i) choose an effective theory to describe the production of the D meson pair, $\gamma\gamma \to D^+D^-$, and (ii) introduce a prescription to form the mesonic bound state. All this was done recently in [21] but only for low energy collisions.

In (I) we have to face the problem of properly considering the QCD corrections in the $\gamma\gamma \to c\bar{c}$ cross section and also include the "resolved photon" contribution as done (only up to the next-to-leading-order (NLO) level) in [25]. In modern language, the photon is treated as a color dipole, and we need to know the dipole-dipole $\to c\bar{c}$ cross section, as done in [30]. Then in both cases we have uncertainties related to the validity of the fragmentation functions and to the scale used in them. Finally, the prescription to bind the mesons together is based on the proximity in phase space of the constituents, as done in [29]. It is mostly based on kinematics and does not include information about the dynamics of the bound state. In all stages of the calculation there are nonperturbative QCD contributions which are difficult to estimate.

In (II) we do not have problems with hadronization or with nonperturbative contributions, since we are from the beginning at the hadronic level. The effective theory is a version of scalar electrodynamics and is very simple. Moreover, the prescription to bind the mesons can be

implemented at the amplitude level and contains more information about the bound state (uses its wave function). The major drawback in this approach is the use of form factors and the cutoff parameters which come along with them. Fortunately, in the present case we could find experimental data, which could be used to fix the cutoff, thereby reducing the uncertainties.

To summarize, both the hadronic and partonic approaches must be developed. Here we work with first one just because in this case it is more convenient. Along this line, we will study the process $\gamma\gamma \to D^+D^-$ with the Lagrangian densities [31]

$$\mathcal{L} = (D_\mu\phi)^*(D^\mu\phi) - m_D^2\phi^*\phi - \frac{1}{4}F_{\mu\nu}F^{\mu\nu}, \tag{1}$$

and

$$\mathcal{L} = -ig_{\gamma D^+D^{*-}}F_{\mu\nu}\epsilon^{\mu\nu\alpha\beta}(D^{*-}_\alpha \overleftrightarrow{\partial_\beta} D^+ + D^- \overleftrightarrow{\partial_\beta} D^{*+}_\alpha), \tag{2}$$

where

$$D_\mu\phi = \partial_\mu\phi + ieA_\mu\phi, \qquad F_{\mu\nu} = \partial_\mu A_\nu - \partial_\nu A_\mu,$$

and ϕ, D^*, and A_μ represent the D^+ (or D^-), the D^{*+} (or D^{*-}), and the photon fields, respectively. The Feynman rules can be derived from the interaction terms, and they yield the Feynman diagrams for the process $\gamma\gamma \to D^+D^-$ shown in Fig. 1. In the figure we also show the quadrimomenta of the incoming photons $k^\mu = (E_p, 0, 0, k)$, $k'^\mu = (E_{k'}, 0, 0, k')$ and of the outgoing mesons $p^\mu = (E_p, 0, 0, p)$, $p'^\mu = (E_{p'}, 0, 0, p')$. The total amplitude is given by

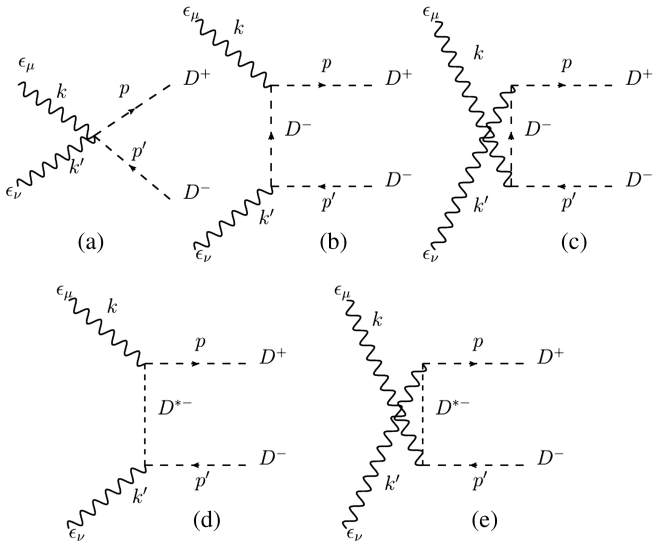

FIG. 1. Feynman diagrams for the process $\gamma\gamma \to D^+D^-$. a) Contact term. b) D exchange in the t-channel. c) D exchange in the u-channel. d) D^* exchange in the t-channel. e) D^* exchange in the u-channel.

$$iM = iM_{(a)} + iM_{(b)} + iM_{(c)} + iM_{(d)} + iM_{(e)}, \tag{3}$$

where

$$iM_{(a)} = 2ie^2 g_{\mu\nu}F(\bar{q}^2)F(\bar{q}^2)\varepsilon^{*\mu}(k)\varepsilon^{*\nu}(k'), \tag{4}$$

$$iM_{(b)} = \varepsilon^{*\mu}(k)ieF(\hat{t})(-2p_\mu + k_\mu)\frac{i}{(k-p)^2 - m_D^2}ieF(\hat{t})(2p'_\nu - k'_\nu)\varepsilon^{*\nu}(k'), \tag{5}$$

$$iM_{(c)} = \varepsilon^{*\mu}(k')ieF(\hat{u})(-2p_\mu + k'_\mu)\frac{i}{(k'-p)^2 - m_D^2}ieF(\hat{u})(2p'_\nu - k_\nu)\varepsilon^{*\nu}(k), \tag{6}$$

$$iM_{(d)} = \varepsilon^*_\mu(k)[-2g\epsilon^{\sigma\mu\alpha\rho}k_\sigma(k_\rho - 2p_\rho)F(\hat{t})]\left[\frac{-i\left(g_{\alpha\beta} - \frac{(k-p)_\alpha(k-p)_\beta}{m^2_{D^*}}\right)}{(k-p)^2 - m^2_{D^*}}\right][2g\epsilon^{\delta\nu\beta\lambda}k'_\delta(-k'_\lambda + 2p'_\lambda)F(\hat{t})]\varepsilon^*_\nu(k'), \tag{7}$$

$$iM_{(e)} = \varepsilon^*_\mu(k')[-2g\epsilon^{\sigma\mu\alpha\rho}k'_\sigma(k'_\rho - 2p_\rho)F(\hat{u})]\left[\frac{-i\left(g_{\alpha\beta} - \frac{(k'-p)_\alpha(k'-p)_\beta}{m^2_{D^*}}\right)}{(k'-p)^2 - m^2_{D^*}}\right][2g\epsilon^{\delta\nu\beta\lambda}k_\delta(-k_\lambda + 2p'_\lambda)F(\hat{u})]\varepsilon^*_\nu(k), \tag{8}$$

where $\bar{q}^2 = [(k-p)^2 + (k'-p)^2]/2$ and $g = g_{\gamma D^+D^{*-}} = -0.035$ [31]. We have introduced the Mandelstam variables of the elementary process, which are $\hat{s} = (k+k')^2$, $\hat{t} = (k-p)^2$, and $\hat{u} = (k'-p)^2$. As usual, we have included form factors, $F(q)$, in the vertices of the above amplitudes. We shall follow [32] and use the monopole form factor given by

$$F(q^2) = \frac{\Lambda^2 - m^2_{D^{(*)}}}{\Lambda^2 - q^2}, \tag{9}$$

where q is the 4-momentum of the exchanged meson and Λ is a cutoff parameter. This choice has the advantage of yielding automatically $F(m_D^2) = 1$ and $F(m_{D^*}^2) = 1$ when the exchanged meson is on shell. The above form is arbitrary, but there is hope to improve this ingredient of the calculation using QCD sum rules to calculate the form factor, as done in [33], thereby reducing the uncertainties. The form factors needed for our calculation are those associated to the vertices $DD\gamma$ and $D^*D\gamma$ and can be calculated with the Shifman-Vainshtein-Zakharov QCD sum rules [34] or with the QCD light cone sum rules [35]. Technical details of the method are given in [33]. The calculation consists of the evaluation of the three point correlation function of three currents, representing the two mesons and the photon. All the ingredients are known, but the calculations, to the best of our knowledge, were never done so far. Other form factors of vertices with photons and mesons (or baryons) were performed, for example, in [36–39].

Taking the square of the amplitude, Eq. (3), and the average over the photon polarizations it is straightforward to calculate the differential cross section:

$$\frac{d\sigma}{d\Omega} = \frac{1}{64\pi^2}\frac{1}{E_{CM}^2}\frac{|\mathbf{p}|}{|\mathbf{k}|}|M(\gamma\gamma \to D^+D^-)|^2. \tag{10}$$

In the center-of-mass reference frame we have $\mathbf{k} = -\mathbf{k}'$ and hence $\mathbf{p} = -\mathbf{p}'$, $E_{CM} = E_k + E_{k'} = 2|\mathbf{k}|$, and $E_{CM} = E_p + E_{p'} = 2\sqrt{|\mathbf{p}|^2 + m_D^2}$. It is then easy to see that

$$\frac{|\mathbf{p}|}{|\mathbf{k}|} = \sqrt{\frac{(E_{CM}^2 - 4m_D^2)/4}{E_{CM}^2/4}} = \sqrt{1 - \frac{4m_D^2}{E_{CM}^2}}. \tag{11}$$

Inserting Eq. (11) into Eq. (10) and using $E_{CM}^2 = \hat{s}$ we find

$$\sigma = \frac{1}{64\pi^2}\frac{1}{\hat{s}}\sqrt{1 - \frac{4m_D^2}{\hat{s}}}\int |M(\gamma\gamma \to D^+D^-)|^2 d\Omega. \tag{12}$$

The angular integral can be done using the relations

$$\hat{t} = m_D^2 - \frac{\hat{s}}{2} + \left(\sqrt{\hat{s}\left(\frac{\hat{s}}{4} - m_D^2\right)}\right)\cos(\theta),$$

$$\hat{u} = m_D^2 - \frac{\hat{s}}{2} - \left(\sqrt{\hat{s}\left(\frac{\hat{s}}{4} - m_D^2\right)}\right)\cos(\theta),$$

where θ is the angle between $\mathbf{k}$ and $\mathbf{p}$. We emphasize that the only unknown in our calculation is the cutoff parameter Λ. In what follows, we will determine it fitting our cross section to the large electron-positron collider (LEP) data on the process $e^+e^- \to e^+e^-c\bar{c}$.

III. PRODUCTION OF BOUND STATES

Now we describe the method to construct a bound state (denoted B) from the D^+D^- pair. As in [10], we impose phase space constraints on the mesons, forcing them to be "close together." Here we do this through the prescription discussed in [40]. The bound state $|B\rangle$ is defined as

$$\frac{|B\rangle}{\sqrt{2E_B}} \equiv \int \frac{d^3q}{(2\pi)^3}\tilde{\psi}^*(\mathbf{q})\frac{1}{\sqrt{2E_q}}\frac{1}{\sqrt{2E_{-q}}}|\mathbf{q}, -\mathbf{q}\rangle, \tag{13}$$

where E_B is the bound state energy, $\mathbf{q}$ is the relative three momentum between D^+ and D^- in the state B, $E_{\pm q}$ are the energies of D^+ and D^-, and $\tilde{\psi}(\mathbf{q})$ is the bound state wave function in momentum space, which has the following properties:

$$\tilde{\psi}(\mathbf{q}) = \int d^3x e^{i\mathbf{q}\cdot\mathbf{x}}\psi(\mathbf{x}); \qquad \int \frac{d^3q}{(2\pi)^3}|\tilde{\psi}(\mathbf{q})|^2 = 1. \tag{14}$$

From Eq. (13), we can write the following relation between the amplitudes:

$$\frac{M(\gamma\gamma \to B)}{\sqrt{2E_B}} = \int \frac{d^3q}{(2\pi)^3}\tilde{\psi}^*(\mathbf{q})\frac{1}{\sqrt{2E_{D^+}}} \times \frac{1}{\sqrt{2E_{D^-}}}M(\gamma\gamma \to D^+D^-). \tag{15}$$

We assume that the $\mathbf{p} \simeq \mathbf{p}'$ and hence $E_{D^+} \simeq E_{D^-} = E_D$ and also $\mathbf{q} = \mathbf{p} - \mathbf{p}' \simeq 0$. Therefore the energy E_D and the amplitude $M(\gamma\gamma \to D^+D^-)$ can be taken out of the integral. Moreover, since the binding energy is small we have $E_B \simeq 2E_D$ and hence

$$\frac{M(\gamma\gamma \to B)}{\sqrt{2E_B}} = \frac{M(\gamma\gamma \to D^+D^-)}{E_B}\int \frac{d^3q}{(2\pi)^3}\tilde{\psi}^*(\mathbf{q}),$$

$$M(\gamma\gamma \to B) = \sqrt{\frac{2}{E_B}}M(\gamma\gamma \to D^+D^-) \times \int \frac{d^3q}{(2\pi)^3}\int d^3x\psi^*(\mathbf{x})e^{i\mathbf{q}\cdot\mathbf{x}},$$

$$= \sqrt{\frac{2}{E_B}}M(\gamma\gamma \to D^+D^-)\int d^3x\psi^*(\mathbf{x})\delta^{(3)}(\mathbf{x}),$$

$$= \psi^*(0)\sqrt{\frac{2}{E_B}}M(\gamma\gamma \to D^+D^-). \tag{16}$$

With the amplitude above we calculate the cross section for bound state production:

$$d\sigma = \frac{1}{H}\frac{d^3p_B}{(2\pi)^3}\frac{1}{2E_B}(2\pi)^4\delta^{(4)}(k + k' - p_B)|M(\gamma\gamma \to B)|^2, \tag{17}$$

where p_B is the momentum of the produced bound state and H is the flux factor. Now we will work in the center of mass frame of the $AA \to AAB$ collision, in which the momenta of the incoming photons may be different. In this frame we have

$$k=(\omega_1,0,0,\omega_1),\qquad k'=(\omega_2,0,0,-\omega_2),\qquad p_B\equiv p+p'=(E_B,0,0,\omega_1-\omega_2), \tag{18}$$

where $E_B=\sqrt{(\omega_1-\omega_2)^2+m_B^2}$ and ω_1 and ω_2 are the energies of the colliding photons. The flux factor is then given by

$$H=4\sqrt{(k\cdot k')^2-m_k^2m_{k'}^2}=4k\cdot k'=4(k_0k_0'-\mathbf{k}\cdot\mathbf{k}')=4(\omega_1\omega_2-\omega_1(-\omega_2))=2(4\omega_1\omega_2). \tag{19}$$

Inserting this expression into Eq. (17) and integrating, the cross section reads as

$$\begin{aligned}\sigma(\omega_1,\omega_2)&=\frac{2\pi}{2(4\omega_1\omega_2)}\int\frac{d^3p_B}{2E_B}\delta(E_{CM}-E_B)\delta^{(3)}(\mathbf{k}+\mathbf{k}'-\mathbf{p}_B)\left[\frac{2}{E_B}|\psi(0)|^2|M(\gamma\gamma\to D^+D^-)|^2\right],\\&=\frac{\pi|\psi(0)|^2}{4\omega_1\omega_2E_B^2}|M(\gamma\gamma\to D^+D^-)|^2\frac{4\omega_1^2+m_B^2}{8\omega_1^2}\delta\left(\omega_2-\frac{m_B^2}{4\omega_1}\right),\end{aligned} \tag{20}$$

where we have used that $E_{CM}^2=4\omega_1\omega_2$.

To proceed with the calculation we need to know the bound state wave function at the origin $|\psi(0)|^2$. Fortunately, in [41] a similar bound state of open charm mesons was studied with the Bethe-Salpeter equation, and an expression for the wave function was derived. In the first part of their paper the authors present a formalism which is general and can be adapted to our system. Formally, the Bethe-Salpeter equation reads as $T=V+VGT$, where T is the two-body amplitude, and V is a matrix with elements V_{ij} which are the amplitudes of the $i\to j$ transitions and which are calculated from a given effective Lagrangian. Finally G is a loop function, which can be regularized with a cutoff. Here we will just quote the main formulas needed to calculate $\psi(0)$, which is given by

$$\psi(0)=\frac{g}{(2\pi)^{3/2}}G, \tag{21}$$

where

$$\begin{aligned}&G=-8\mu\pi\left(\Lambda_0-\gamma\arctan\left(\frac{\Lambda_0}{\gamma}\right)\right),\\&\gamma=\sqrt{2\mu E_b},\quad g^2=\frac{\gamma}{8\pi\mu^2\left(\arctan\left(\frac{\Lambda_0}{\gamma}\right)-\frac{\gamma\Lambda_0}{\gamma^2+\Lambda_0^2}\right)}.\end{aligned} \tag{22}$$

In the above expressions μ is the reduced mass ($\mu=m_D/2$), Λ_0 is a cutoff parameter, and E_b is the binding energy. We shall follow [22] and assume that $\Lambda_0=1$ GeV. From the above equations we see that one can compute the (dynamically generated) mass of a bound state and then determine its binding energy. Knowing μ, E_b and fixing Λ_0, we can use the above formulas to calculate $\psi(0)$. In what follows our reference value will be obtained using $m_D=1870$ MeV and the mass of the bound state equal to $M_B=3723$ MeV, as found in [22]. With these numbers we get $E_b=17$ MeV and $|\psi(0)|^2=0.008$ GeV^3. These will be the values used to obtain all results, unless stated otherwise.

IV. EQUIVALENT PHOTON APPROXIMATION AND THE NUMBER OF PHOTONS

The equivalent photon approximation is well known, and it is described in several papers [6,42]. In general, when the photon source is a nucleus one has to use form factors, and the calculation becomes somewhat complicated. Here we will follow [6] and define an UPC in momentum space. The distribution of equivalent photons generated by a moving particle with the charge Ze is [6]:

$$n(\mathbf{q})d^3q=\frac{Z^2\alpha}{\pi^2}\frac{(\mathbf{q}_\perp)^2}{\omega q^4}d^3q=\frac{Z^2\alpha}{\pi^2\omega}\frac{(\mathbf{q}_\perp)^2}{((\mathbf{q}_\perp)^2+(\omega/\gamma)^2)^2}d^3q, \tag{23}$$

where $\alpha=e^2/(4\pi)$, q is the photon 4-momentum, $\mathbf{q}_\perp$ is its transverse component, ω is the photon energy and γ is the Lorentz factor of the photon source ($\gamma=\sqrt{s}/2m_p$ and m_p is the proton mass). To obtain the equivalent photon spectrum, one has to integrate this expression over the transverse momentum up to some value $\hat{q}$. The value of $\hat{q}$ is given by $\hat{q}=\hbar c/2R$, where R is the radius of the projectile. For Pb, $R\approx 7$ fm, and hence $\hat{q}\approx 0.014$ GeV. After the integration over the photon transverse momentum the equivalent photon energy spectrum is given by

$$n(\omega)d\omega=\frac{2Z^2\alpha}{\pi}\ln\left(\frac{\hat{q}\gamma}{\omega}\right)\frac{d\omega}{\omega}. \tag{24}$$

Because of the approximations the above distribution is valid when the condition $\omega\ll\hat{q}\gamma$ is fulfilled. Using Eq. (24) we can compute the cross sections of free pair production, σ_P, and of bound state production, σ_B. They are given by

$$\sigma_P(AA \to AAD^+D^-) = \int_{m_D^2/\hat{q}\gamma}^{\hat{q}\gamma} d\omega_1 \int_{m_D^2/\omega_1}^{\hat{q}\gamma} d\omega_2 \sigma_P(\omega_1,\omega_2) n(\omega_1) n(\omega_2), \quad (25)$$

$$\sigma_B(AA \to AAB) = \int_{m_D^2/\hat{q}\gamma}^{\hat{q}\gamma} d\omega_1 \int_{m_D^2/\omega_1}^{\hat{q}\gamma} d\omega_2 \sigma_B(\omega_1,\omega_2) n(\omega_1) n(\omega_2), \quad (26)$$

where $\sigma_P(\omega_1,\omega_2)$ and $\sigma_B(\omega_1,\omega_2)$ are given by Eq. (12) (with $\hat{s} = 4\omega_1\omega_2$) and (20) respectively.

V. THE LOW ENERGY APPROXIMATION

A. Free pairs

At low photon energies and close to the D^+D^- threshold, the produced mesons are nonrelativistic, and we can use the approximation $k - p \approx (0,0,0,m_D)$ in the heavy meson propagator, i.e.,

$$\frac{1}{(k-p)^2 - m_D^2} \approx \frac{1}{0 - m_D^2 - m_D^2} = \frac{-1}{2m_D^2}.$$

An analogous expression can be written for the D^* propagator. From the above relation we can see that in this low energy regime the amplitudes with propagators are proportional to $\propto 1/m_D^2$ [Figs. 1(b) and 1(c)] and $\propto 1/m_D^{*2}$ [Figs. 1(d) and 1(e)] and can be neglected when compared to the amplitudes without propagators, such as the one of the contact interaction in Fig. 1(a). With this approximation the amplitude for D^+D^- production in the process $\gamma\gamma \to D^+D^-$ is given by

$$iM(\gamma\gamma \to D^+D^-) \approx 2ie^2F^2(-m_D^2) g_{\mu\nu}\varepsilon^{*\mu}(k)\varepsilon^{*\nu}(k'). \quad (27)$$

Taking the square and performing the average over the photon polarizations we have

$$|M(\gamma\gamma \to D^+D^-)|^2 = \frac{1}{4}\sum_{\text{pol}} 2ie^2F^2(-m_D^2) g_{\mu\nu}\varepsilon^{*\mu}(k)\varepsilon^{*\nu}(k')(-2ie^2)F^2(-m_D^2) g_{\sigma\rho}\varepsilon^{\sigma}(k)\varepsilon^{\rho}(k'),$$
$$= e^4F^4(-m_D^2) g_{\mu\nu}g_{\sigma\rho}g^{\mu\sigma}g^{\nu\rho} = 4e^4F^4(-m_D^2). \quad (28)$$

Inserting this amplitude into Eq. (10) we find

$$\frac{d\sigma}{d\Omega} = \frac{e^4F^4(-m_D^2)}{16\pi}\frac{1}{E_{CM}^2}\sqrt{1 - \frac{4m_D^2}{E_{CM}^2}}. \quad (29)$$

Performing the integral over the solid angle and using the definitions $\alpha \equiv e^2/4\pi$ and $E_{CM}^2 = 4\omega_1\omega_2$, we find

$$\sigma(\omega_1,\omega_2) = \frac{\pi\alpha^2F^4(-m_D^2)}{\omega_1\omega_2}\sqrt{1 - \frac{m_D^2}{\omega_1\omega_2}}, \quad (30)$$

which is then substituted in Eq. (25) to give the final cross section for $AA \to AAD^+D^-$.

B. Bound states

In the low energy approximation the produced bound state is nonrelativistic, and then Eq. (16) reduces to

$$M(\gamma\gamma \to B) = \psi^*(0)\sqrt{\frac{2}{m_B}} M(\gamma\gamma \to D^+D^-). \quad (31)$$

Inserting Eq. (28) into the above equation and then using it in Eq. (20) we have

$$\sigma(\omega_1,\omega_2) = \frac{32\pi^3\alpha^2F^4(-m_D^2)|\psi(0)|^2}{m_B}\frac{1}{\omega_1\omega_2}\delta(4\omega_1\omega_2 - E_B^2). \quad (32)$$

Substituting the above expression into Eq. (26) and integrating we obtain the final analytical expression:

$$\sigma_B(AA \to AAB) = \frac{256\pi|\psi(0)|^2Z^4\alpha^4F^4(-m_D^2)}{3m_B^5} \times \left[\ln\left(\frac{s\hat{q}^2}{m_p^2m_B^2}\right)\right]^3. \quad (33)$$

We emphasize that "low energy" here refers to the energy released by the projectiles, i.e., the invariant mass of the photon pair. The nuclear projectiles themselves may have very high energies.

VI. NUMERICAL RESULTS AND DISCUSSION

Having derived all the main formulas and discussed the numerical inputs, now we present our numerical results. In Fig. 2 we show the cross sections for free pair production and compare it to the existing experimental data from LEP [43]. In fact, the LEP data are for $e^+e^- \to e^+e^-c\bar{c}$, i.e., the measured final states are D^+D^- and $D^0\bar{D}^0$. We assume that these two final states have the same cross section, and, in

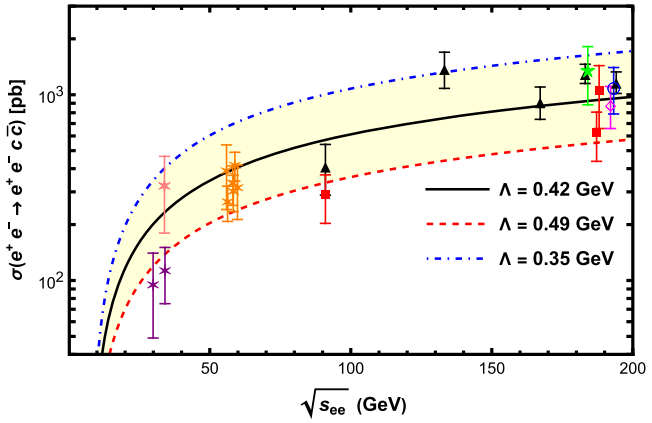

FIG. 2. Cross section for the process $e^+e^- \to c\bar{c}$ as a function of the energy $\sqrt{s}$ measured by the LEP Collaborations. Data are from Ref. [43]. The purple stars are from TASSO, the pale red single star is from JADE, the bright orange stars are from TOPAZ, AMY, and VENUS, the triangles are from L3, the squares and the green star are from ALEPH, the single diamond is from DELPHI, and the circle is from OPAL. The curves are calculated with Eqs. (12) and (25).

order to compare with the data, we multiply our cross section $\sigma(e^+e^- \to e^+e^-D^+D^-)$ by a factor of 2. In order to fit these data we will adapt expression (25) to electron-positron collisions. The $\gamma\gamma \to D^+D^-$ cross section is the same, but the photon flux from the electron (and also from the positron) and the integration limits are different. The adaptation of Eq. (25) is performed in the Appendix. Comparing our formula with these data, we determine the only parameter in the calculation, which is the cutoff Λ. In the figure, the curves are obtained substituting Eqs. (12) and (A3) into (25). In the latter $\hat{q} = m_e$. We did not attempt to perform a least chi square fit. Instead we will carry on some uncertainty and work with the band $0.35 < \Lambda < 0.49$ GeV.

In Fig. 3 we show the cross section for D^+D^- production. The black solid lines show the result with our central parameter choice. Figure 3(a) shows the sensitivity of the result to the value of $\hat{q}$. In Fig. 3(b) we vary the values of Λ in the range defined in Fig. 2. In this sense we propagate the uncertainty from the fit of the data to our results. Taking this as the error in our result, the obtained cross section for

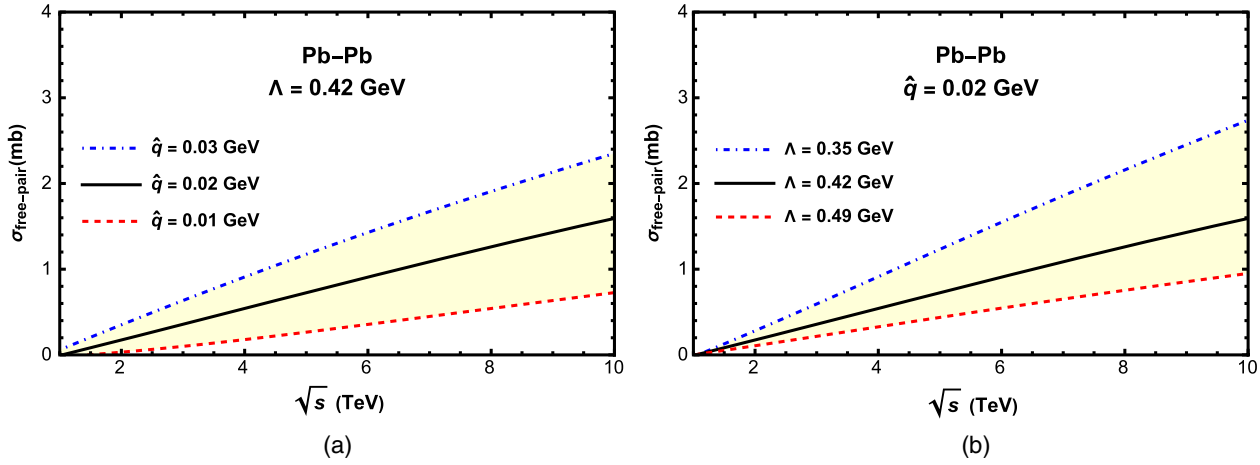

FIG. 3. Cross sections for free D^+D^- pair production as a function of the energy $\sqrt{s}$. (a) Dependence on $\hat{q}$ for fixed Λ. (b) Dependence on Λ for fixed $\hat{q}$.

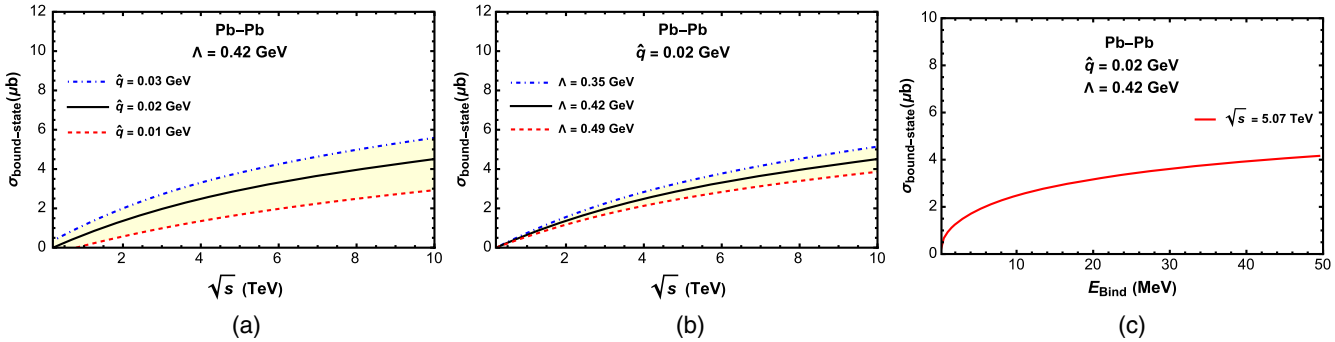

FIG. 4. Cross sections for D^+D^- bound state production as a function of the energy $\sqrt{s}$. (a) Dependence on $\hat{q}$ for fixed Λ. (b) Dependence on Λ for fixed $\hat{q}$. (c) Dependence on the binding energy for fixed Λ and $\hat{q}$.

TABLE I. Cross sections for exotic meson production in ultraperipheral $Pb-Pb$ collisions at $\sqrt{s_{NN}} = 5.5$ TeV obtained in [4]. The three cross sections refer to the use of three different nuclear form factors, as explained in [4].

State	Mass	$\Gamma_{\gamma\gamma}^{\text{theor}}$(keV)	$\sigma_{b_{\min}}(\mu b)$	$\sigma_F(\mu b)$	$\sigma_R(\mu b)$
X(3915), 0^{++}	3919	0.20	5.1	7.3	6.7
X(3940), 0^{++}	3943	0.33	8.2	11.8	10.8
X(4140), 0^{++}	4143	0.63	12.9	18.7	17.1

the reaction $PbPb \to PbPbD^+D^-$ at $\sqrt{s_{NN}} = 5.02$ TeV is

$$\sigma(PbPb \to PbPbD^+D^-) = 0.75^{+0.4}_{-0.4} \text{ mb}. \quad (34)$$

Assuming that the reaction $PbPb \to PbPbD^0\bar{D}^0$ has the same cross section as the one given above for charged states and neglecting other final states, such as D^*, the total cross section for charm production in photon-photon exclusive processes, we have

$$\sigma_{\text{exclusive}}(PbPb \to PbPbc\bar{c}) = 1.5^{+0.4}_{-0.4} \text{ mb}. \quad (35)$$

In Ref. [30] a similar calculation was performed. The authors studied open charm production in ultraperipheral $PbPb$ collisions at $\sqrt{s_{NN}} = 5.5$ TeV. They considered the mechanisms of $c\bar{c}$ production mentioned above, i.e., direct production, NLO QCD corrections, and the resolved photon contribution. They did not include the hadronization of the charm quarks, i.e., $c \to D$ and $\bar{c} \to \bar{D}$. The final cross section was found to be 2.47 mb. Given that they considered more processes and also that they used an energy $\sqrt{s_{NN}}$ higher than ours, we can conclude that both cross sections are compatible with each other.

In Fig. 4 we present the cross section for bound state production and study its dependence on $\hat{q}$ [Fig. 4(a)], on Λ [Fig. 4(b)], and on the binding energy E_b [Fig. 4(c)]. As expected, it is much smaller than the cross section for open free pair production. However, it is encouraging to see that at $\sqrt{s_{NN}} \approx 5.02$ TeV we have

$$\sigma(PbPb \to PbPbB) = 3.0^{+0.8}_{-1.2} \ \mu\text{b}. \quad (36)$$

This number could be compared with results found in [4] and in [5]. In those papers, the production cross section of the scalar molecular states in $PbPb$ at $\sqrt{s_{NN}} = 5.5$ TeV were calculated, and the results are shown in Table I.

The work [4] (and also [5]) is relevant for us because there the multiquark states were also treated as molecules. Indeed, the widths listed in Table I were theoretically calculated in a formalism in which the constituent mesons interact and a resonance (or bound state) is dynamically generated. However there are important differences. First, the energy used in [4] is higher than the one used here, and hence the cross sections are higher. Also, the states $X(3940)$ and $X(3915)$ are significantly heavier than the D^+D^- molecule, whose mass is 3723 MeV. Moreover, in [4] the equivalent photon calculation was done in the impact parameter space with the use of nuclear form factors. In spite of these differences the obtained cross sections are of the same order of magnitude.

Another interesting comparison can be made between the cross section (36) and the result obtained in [7], where the authors study the $J^{PC} = 0^{++}$ state (which they call X_0 with $m_{X_0} = 3770$ MeV) which was predicted by the tetraquark (diquark-antidiquark) model in Ref. [8]. They use the same formalism as in [4,5], and the X_0 production cross section turns out to be $\sigma_{X_0} \simeq 0.18$ μb. This a is an order of magnitude smaller than (36). This difference is a direct consequence of the two-photon decay width, which in [7] was estimated to be $\Gamma_{\gamma\gamma} \simeq 6.3$ eV, a value 100 times (or more) smaller than those quoted in Table I. This discrepancy challenges the expectation described in the Introduction and deserves further studies.

For completeness, in Fig. 5(a) we compare the cross sections for free pair and bound state production, and in Fig. 5(b) we compare the exact numerical evaluation of σ_B with the approximate analytical expression, Eq. (33). We observe that the cross section obtained with the analytical formula is accurate only at low energies. At higher energies

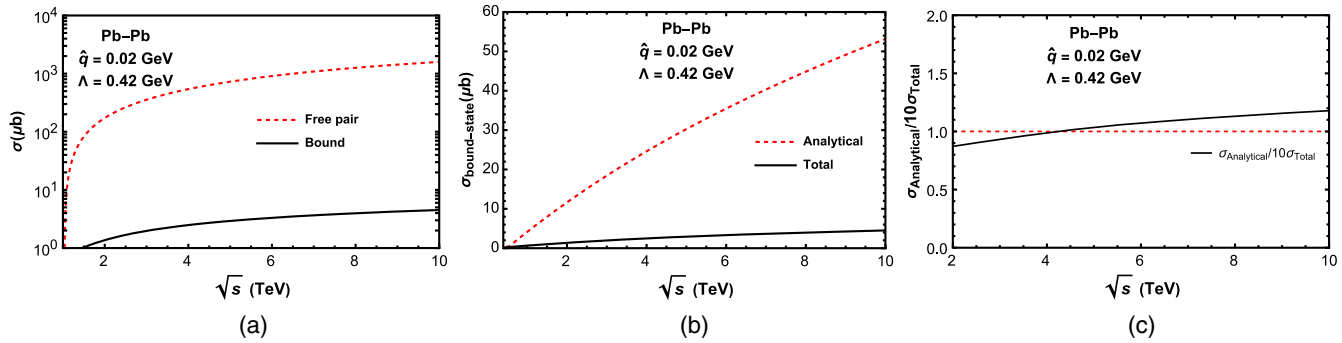

FIG. 5. Cross sections as a function of $\sqrt{s}$. (a) Comparison between the free D^+D^- pair and bound state B cross sections. (b) Comparison between the complete numerical solution and the approximate analytical cross section. (c) Ratio between the cross section.

it becomes larger than the complete numerical formula. We can understand this behavior noticing that in Eq. (33) we assumed that both E_B and the form factor $F(q^2)$ did not depend on ω_1 nor on ω_2 at low energies and therefore resulted in a smaller denominator (m_B where it should have been E_B) and a constant argument of the form factor, which, as we can see from Fig. 4(b), is crucial to our numerical results. Nevertheless, the exact and the analytical formula differ essentially only by a multiplicative factor close to 10. Dividing Eq. (33) by 10, it reproduces the exact formula within 20% accuracy in the relevant LHC range and can thus be useful for practical applications. This is shown Fig. 5(c).

To summarize, we have calculated the cross section for the production of a heavy meson molecule in ultraperipheral collisions. We have combined a effective Lagrangian to compute the amplitude of the process $\gamma\gamma \to D^+D^-$ with a prescription to project this amplitude onto the amplitude for bound state formation. The resulting $\gamma\gamma \to B$ cross section was then convoluted with the equivalent photon fluxes from the projectile and target, and the final cross section $\sigma_B(AA \to AAB)$ was obtained. For $\sqrt{s_{NN}} = 5.02$ TeV it is $3.0^{+0.8}_{-1.2}$ μb. This number is consistent with the results obtained for other scalar exotic charmonium molecules in [4,5]. The parameters of the calculation are Λ, $\hat{q}$, and E_b, which are the hadronic form factor cutoff, the maximum momentum of an emitted photon and the binding energy, respectively. All these parameters can be constrained by experimental information and by calculations. Thus, we believe that in the future it will be possible to increase the precision of our calculation.

ACKNOWLEDGMENTS

We are deeply indebted to K. Khemchandani and A. Martinez Torres for instructive discussions. We are also grateful to A. Esposito for bringing Ref. [7] to our attention. This work was partially financed by the Brazilian funding agencies CNPq, CAPES, FAPESP, FAPERGS, and INCT-FNA (Process No. 464898/2014-5). F. S. N. gratefully acknowledges the support from the Fundação de Amparo à Pesquisa do Estado de São Paulo (FAPESP). C. A. B. acknowledges support by the U.S. DOE Grant No. DE-FG02-08ER41533 and the Helmholtz Research Academy Hesse for FAIR.

APPENDIX: CROSS SECTION OF THE PROCESS $e^+e^- \to e^+e^-D^+D^-$

In this appendix we will adapt Eq. (25) to the $e^+e^- \to e^+e^-c\bar{c}$ process. We start from Eq. (23) with $Z = 1$:

$$n(\mathbf{q})d^3q = \frac{\alpha}{\pi^2\omega}\frac{(\mathbf{q}_\perp)^2}{((\mathbf{q}_\perp)^2 + (\omega/\gamma)^2)^2}d^3q. \quad \text{(A1)}$$

First we recall that $d^3q = dq_x dq_y dq_z = q_\perp dq_\perp d\theta dq_z = 1/2 dq_\perp^2 d\theta dq_z \to \pi dq_\perp^2 dq_z$. Then we make the following change of variables:

$$dq_\perp^2 dq_z = \frac{\omega}{\sqrt{\omega^2 - q_\perp^2}}dq_\perp^2 d\omega.$$

After changing the variables we integrate Eq. (A1) over $q_\perp^2$:

$$n(\omega) = \frac{\alpha}{\pi}\int_0^{\omega^2}\frac{q_\perp^2}{[q_\perp^2 + (\omega/\gamma)^2]^2}\frac{1}{\sqrt{\omega^2 - q_\perp^2}}dq_\perp^2. \quad \text{(A2)}$$

The solution of this integral is

$$n(\omega) = \frac{\alpha}{\pi}\frac{1}{\omega}\frac{\gamma}{(1+\gamma^2)^{3/2}} \times \left[2\gamma^2\text{arcsinh}(\gamma) + \text{arcsinh}(\gamma) - \gamma\sqrt{1+\gamma^2}\right]. \quad \text{(A3)}$$

After these changes in Eq. (25), we can write the cross section for the process $e^+e^- \to e^+e^-D^+D^-$ inserting Eq. (A3) into Eq. (25) and recalling that for electrons we use $\gamma = \sqrt{s}/2m_e$ and also $\hat{q} = m_e$.

[1] N. Brambilla, S. Eidelman, C. Hanhart, A. Nefediev, C.-P. Shen, C. E. Thomas, A. Vairo, and C.-Z. Yuan, Phys. Rep. **873**, 1 (2020); R. M. Albuquerque, J. M. Dias, K. P. Khemchandani, A. Martinez Torres, F. S. Navarra, M. Nielsen, and C. M. Zanetti, J. Phys. G **46**, 093002 (2019).
[2] L. Meng, B. Wang, G. J. Wang, and S. L. Zhu, Phys. Rep. **1019**, 1 (2023).
[3] C. A. Bertulani, S. Klein, and J. Nystrand, Annu. Rev. Nucl. Part. Sci. **55**, 271 (2005).
[4] B. D. Moreira, C. A. Bertulani, V. P. Goncalves, and F. S. Navarra, Phys. Rev. D **94**, 094024 (2016).
[5] R. Fariello, D. Bhandari, C. A. Bertulani, and F. S. Navarra, Phys. Rev. C **108**, 044901 (2023).
[6] C. A. Bertulani and G. Baur, Phys. Rep. **163**, 299 (1988).
[7] A. Esposito, C. A. Manzari, A. Pilloni, and A. D. Polosa, Phys. Rev. D **104**, 114029 (2021).
[8] L. Maiani, F. Piccinini, A. D. Polosa, and V. Riquer, Phys. Rev. D **89**, 114010 (2014).

[9] D. Marietti, A. Pilloni, and U. Tamponi, Phys. Rev. D **106**, 094040 (2022); S. J. Brodsky and F. S. Navarra, Phys. Lett. B **411**, 152 (1997).
[10] P. Artoisenet and E. Braaten, Phys. Rev. D **83**, 014019 (2011); **81**, 114018 (2010); C. Bignamini, B. Grinstein, F. Piccinini, A. D. Polosa, and C. Sabelli, Phys. Rev. Lett. **103**, 162001 (2009).
[11] A. Esposito, E. G. Ferreiro, A. Pilloni, A. D. Polosa, and C. A. Salgado, Eur. Phys. J. C **81**, 669 (2021).
[12] H. Zhang, J. Liao, E. Wang, Q. Wang, and H. Xing, Phys. Rev. Lett. **126**, 012301 (2021); B. Wu, X. Du, M. Sibila, and R. Rapp, Eur. Phys. J. A **57**, 122 (2021).
[13] D. Gamermann, E. Oset, D. Strottman, and M. J. Vicente Vacas, Phys. Rev. D **76**, 074016 (2007).
[14] J. Nieves and M. P. Valderrama, Phys. Rev. D **86**, 056004 (2012).
[15] C. Hidalgo-Duque, J. Nieves, and M. P. Valderrama, Phys. Rev. D **87**, 076006 (2013).
[16] S. Prelovsek, S. Collins, D. Mohler, M. Padmanath, and S. Piemonte, J. High Energy Phys. 06 (2021) 035.
[17] D. Gamermann and E. Oset, Eur. Phys. J. A **36**, 189 (2008).
[18] P. Pakhlov *et al.* (Belle Collaboration), Phys. Rev. Lett. **100**, 202001 (2008).
[19] K. Chilikin *et al.* (Belle Collaboration), Phys. Rev. D **95**, 112003 (2017).
[20] E. Wang, W.-H. Liang, and E. Oset, Eur. Phys. J. A **57**, 38 (2021).
[21] E. Wang, H.-S. Li, W.-H. Liang, and E. Oset, Phys. Rev. D **103**, 054008 (2021).
[22] C. W. Xiao and E. Oset, Eur. Phys. J. A **49**, 52 (2013).
[23] O. Deineka, I. Danilkin, and M. Vanderhaeghen, Phys. Lett. B **827**, 136982 (2022).
[24] P. C. S. Brandão, J. Song, L. M. Abreu, and E. Oset, Phys. Rev. D **108**, 054004 (2023).
[25] M. Drees, M. Kramer, J. Zunft, and P. M. Zerwas, Phys. Lett. B **306**, 371 (1993).
[26] J. Binnewies, B. A. Kniehl, and G. Kramer, Phys. Rev. D **53**, 6110 (1996).
[27] J. Binnewies, B. A. Kniehl, and G. Kramer, Phys. Rev. D **58**, 014014 (1998).
[28] S. Frixione, M. Krämer, and E. Laenen, Nucl. Phys. **B571**, 169 (2000).
[29] C. Bignamini, B. Grinstein, F. Piccinini, A. D. Polosa, and C. Sabelli, Phys. Rev. Lett. **103**, 162001 (2009).
[30] M. Klusek-Gawenda, A. Szczurek, M. V. T. Machado, and V. G. Serbo, Phys. Rev. C **83**, 024903 (2011).
[31] X. H. Cao, M. L. Du, and F. K. Guo, arXiv:2401.16112.
[32] P. Lebiedowicz, O. Nachtmann, and A. Szczurek, Phys. Rev. D **98**, 014001 (2018).
[33] M. E. Bracco, M. Chiapparini, F. S. Navarra, and M. Nielsen, Prog. Part. Nucl. Phys. **67**, 1019 (2012); F. Carvalho, F. O. Duraes, F. S. Navarra, and M. Nielsen, Phys. Rev. C **72**, 024902 (2005).
[34] M. A. Shifman, A. I. Vainshtein, and V. I. Zakharov, Nucl. Phys. **B147**, 385 (1979); **B147**, 448 (1979).
[35] P. Colangelo and A. Khodjamirian, QCD sum rules, a modern perspective, in *At The Frontier of Particle Physics* (World Scientific, Singapore, 2001).
[36] Y. J. Shi, Z. P. Xing, and U. G. Meißner, Eur. Phys. J. C **83**, 224 (2023).
[37] H. I. Alrebdi and T. Barakat, Universe **7**, 255 (2021).
[38] S. P. Guo, Y. J. Sun, W. Hong, Q. Huang, and G. H. Zhao, Nucl. Phys. **B955**, 115053 (2020).
[39] M. Nielsen and C. M. Zanetti, Phys. Rev. D **82**, 116002 (2010).
[40] *An Introduction to Quantum Field Theory*, edited by M. Peskin and M. Schroeder (Addison-Wesley, Reading, MA, 1996), p. 150.
[41] D. Gamermann, J. Nieves, E. Oset, and E. Ruiz Arriola, Phys. Rev. D **81**, 014029 (2010).
[42] G. Baur, K. Hencken, D. Trautmann, S. Sadovsky, and Y. Kharlov, Phys. Rep. **364**, 359 (2002).
[43] W. Da Silva (DELPHI Collaboration), Nucl. Phys. B, Proc. Suppl. **126**, 185 (2004); A. Csilling (OPAL Collaboration), AIP Conf. Proc. **571**, 276 (2001).